optica

Spectral multiphoton effects and quantum anharmonicities in dissipative cavity-QED systems via off-resonant coherent excitation: supplementary information

E. Illes, C. Roy, and S. Hughes*

Department of Physics, Queen's University, Kingston, Ontario K7L 3N6, Canada

**Corresponding author: shughes@physics.queensu.ca*

Published 31 July 2015

This document provides supplementary information to "Spectral multiphoton effects and quantum anharmonicities in dissipative cavity-QED systems via off-resonant coherent excitation," http://dx.doi.org/10.1364/optica.2.000689. First, we derive the three-state dressed state eigenenergies presented in the main text. Secondly, we use a polaron master equation approach to investigate the role of electron-phonon coupling on the multiphoton spectral features.
http://dx.doi.org/10.1364/optica.2.000689.s001

S1. DRESSED STATE EIGENENERGIES

Here we derive the analytical formula for the dressed state energies of the cavity-QED system Hamiltonian, $H = \hbar\Delta_{xL}\hat{\sigma}^+\hat{\sigma}^- + \hbar\Delta_{cL}\hat{a}^\dagger\hat{a} + \hbar g(\hat{a}^\dagger\hat{\sigma}^- + \hat{\sigma}^+\hat{a}) + \hbar\eta_x(\hat{\sigma}^+ + \hat{\sigma}^-) + +\hbar\eta_c(\hat{a}^\dagger + \hat{a})$, where the various terms are defined in the main paper. In the Jaynes-Cumming (JC) weak excitation approximation (WEA), in which we allow at most one quantum excitation in the system (i.e., a three-state approximation), the Hamiltonian can be written in matrix form

$$H = \begin{pmatrix} 0 & \eta_x & 0 \\ \eta_x & \Delta_L & g \\ 0 & g & \Delta_L \end{pmatrix}, \tag{S1}$$

in the basis $\{|0g\rangle, |0e\rangle, |1g\rangle\}$ (see main paper). Calculating the dressed state energies is equivalent to solving the eigenvalue problem $\det(H - EI) = 0$, with the characteristic equation

$$E^3 - 2\Delta_L E^2 + (\Delta_L^2 - g^2 - \eta_x^2)E + \Delta_L\eta_x^2 = 0. \tag{S2}$$

We identify $b = -2\Delta_L$, $c = \Delta_L^2 - g^2 - \eta_x^2$ and $d = \Delta_L\eta_x^2$ to obtain the general cubic $E^3 + bE_c^2E + d = 0$. The roots of this cubic represent the dressed state energies, and can be obtained using Cardano's method [1]. This entails using two different substitutions in order to make the problem more tenable. First the depressed form of the cubic can be obtained via the substitution $E = z - b/3$. Then making the substitution $z = 2\delta\cos(\theta)$, with $\delta^2 = (b^2 - 3c)/9$ and $y_N = 2b^3/27 - bc/3 + d$, we obtain the form

$$\begin{aligned} 2\delta^3[4\cos^3(\theta) - 3\cos(\theta)] + y_N &= 0 \\ 2\delta^3[\cos(3\theta)] + y_N &= 0, \end{aligned} \tag{S3}$$

after making use of a triple-angle trigonometric identity. This has three unique solutions, giving us the roots

$$E_k = -b/3 + 2\delta\cos(2k\pi/3 + \theta), \tag{S4}$$

with $k = 0, 1, 2$. These are also presented in the main text of the paper in terms of the original variables.

S2. INFLUENCE OF ELECTRON-PHONON COUPLING

In the simple two-level cavity-QED model presented in the main text, we have neglected to take into consideration the role of electron acoustic-phonons scattering for the QD, apart from including a pure dephasing process on the zero phonon line. Even without cavity coupling, the effects of the acoustic phonon bath on the optical properties of QDs is well known [3–5], and characteristic acoustic sidebands appear in the absorption spectrum. This is because the phonon-interactions dress the QD exciton levels to form bands, caused by a nonperturbative coupling of the exciton with the continuum of acoustic phonons. The phonon bath-induced spectral lineshape is elegantly described by the independent boson model (IBM) [6–9], which shows good agreement with single QD emission experiments.

In the nonlinear optics domain, EID (excitation-induced dephasing) occurs due to the interaction of the laser with the underlying acoustic phonon reservoir [7, 10–13]. Recently, Roy and Hughes [14] developed a time-convolutionless master equation to describe coherently driven QD-cavity systems in the presence of the acoustic phonon bath. This polaron-transformed master equation [15], in appropriate limits, formally recovers both the IBM and the JC model. It was found that phonon interactions results in two key effects: (*i*) nonperturbative cavity-exciton coupling, and (*ii*) a systematic dephasing (broadening) of the Mollow triplet peaks—in agreement with experiments using QD micropillars [19]. In the linear excitation regime, and using incoherent excitation, electron-phonon scattering results in an asymmetric vacuum Rabi splitting [15–18] and off-resonant cavity feeding [16, 17, 20–25].

Here we will use the cavity-QED polaron master equation [14] to compute a range of exciton and cavity emitted spectra and show that the main spectral peaks remain robust with respect to phonon coupling, though the general features are less clear and broadened with phonon interactions. As an example, in the main paper we examined multiphoton effects for cavity driven systems, for parameters appropriate for describing semiconductor systems. Here, we include the effects of electron-acoustic phonon coupling to the N-th order and verify that the multiphoton effects we predict are retained with this more complete theoretical treatment for semiconductor QDs.

We will use the polaron-transformed master equation to compare with some of the predictions above for a simple two-level system. The accuracy of this approach has also recently been tested on photoluminescence (PL) intensity emission with a coherently excited system [26], for Mollow triplet data as a function of laser detuning [27], and for explaining phonon-mediated population inversion [28–30]. We highlight that this master equation approach [14] allows one to study the effects of phonons on the cavity emissions by including electron-acoustic phonon coupling to all orders. We will utilize parameter set-A as described in the main text (where $\Gamma_c = g, \Gamma_x = g/100, \Gamma' = g/50$), since it is most representative of current experiments in semiconductor systems in which these interactions are relevant. Following Ref. [14], in order to account for the exciton-phonon interaction, two additional terms are included in the Hamiltonian, via

$$H_p = \sum_q \hbar\omega_q \hat{b}_q^\dagger \hat{b}_q + \hat{\sigma}^+\hat{\sigma}^- \sum_q \hbar\lambda_q(\hat{b}_q + \hat{b}_q^\dagger), \qquad \textbf{(S5)}$$

where $\hat{b}_q^\dagger$ and $\hat{b}_q$ create and annihilate phonons with energy ω_q, respectively, and λ_k (assumed real) is the electron-phonon coupling strength. The first term above describes the free energy of the phonon occupations, and the second describes the coupling between the phonon bath and the exciton. The modified Hamiltonian becomes $\tilde{H} = H + H_p$, where H is given as before by $H = \hbar\Delta_{xL}\hat{\sigma}^+\hat{\sigma}^- + \hbar\Delta_{cL}\hat{a}^\dagger\hat{a} + \hbar g(\hat{a}^\dagger\hat{\sigma}^- + \hat{\sigma}^+\hat{a}) + \hbar\eta_x(\hat{\sigma}^+ + \hat{\sigma}^-) + +\hbar\eta_c(\hat{a}^\dagger + \hat{a})$. Upon undergoing a polaron transformation, $H' = \exp(S)\tilde{H}\exp(-S)$, with $S = \hat{\sigma}^+\hat{\sigma}^-\sum_k \hbar\lambda_k(\hat{b}_q - \hat{b}_q^\dagger)$, we obtain a modified system Hamiltonian,

$$H'_{\rm sys} = \hbar(\Delta_L - \Delta_P)\hat{\sigma}^+\hat{\sigma}^- + \Delta_L\hat{a}^\dagger\hat{a} + +\hbar\eta_c(\hat{a} + \hat{a}^\dagger) + \langle B\rangle X_g, \qquad \textbf{(S6)}$$

where $X_u = \hbar g(\hat{a}^\dagger\hat{\sigma}^- + \hat{a}\hat{\sigma}^+) + \hbar\eta_x(\hat{a}\hat{\sigma}^+ + \hat{a}^\dagger\hat{\sigma}^-)$, $X_g = i\hbar g(\hat{a}^\dagger\hat{\sigma}^- - \hat{a}\hat{\sigma}^+) + i\hbar\eta_x(\hat{a}\hat{\sigma}^+ - \hat{a}^\dagger\hat{\sigma}^-)$, and the polaron shift given by $\Delta_P = \int_0^\infty \frac{J(\omega)}{\omega}$. The spectral function, $J(\omega)$, characterizes the electron-phonon interaction. As seen above, parts of the original Hamiltonian, namely the dot-cavity coupling strength, g, and the pump rate of the driving laser, η_x, are renormalized by a temperature dependent Frank-Condon factor $\langle B\rangle$. This mean phonon displacement operator, at temperature T, is given by $\langle B\rangle = \exp\left[-\frac{1}{2}\int_0^\infty d\omega \frac{J(\omega)}{\omega^2}\coth(\hbar\omega/2k_BT)\right]$, where we have used $\langle B\rangle = \langle B_+\rangle = \langle B_-\rangle$, with $\hat{B}_\pm = \exp[\pm\sum_q \lambda_q/\omega_q(\hat{b}_q - \hat{b}_q^\dagger)]$.

The major phonon interactions for InGaAs QDs are due to the deformation potential [31], which can be represented by the spectral function, $J(\omega) = \alpha_p\,\omega^3\exp(-\omega^2/2\omega_b^2)$. Considering InGaAs QDs, we use phonon coupling parameters estimated by McCutcheon *at al.* [32] from the experiments of Ramsay et al. [11, 12], where $\omega_b = 1$ meV and $\alpha_p/(2\pi)^2 = 0.027$ [11, 12, 32]; larger values of α_p have been reported [17], though these numbers vary in the literature (e.g., see discussions in Ref. [17]).

We next introduce the time-convolutionless (i.e., where $\rho(t)$ is local in time) for the reduced density operator, $\rho(t)$, of the cavity-QED system [15, 32]. In the interaction picture described by $H'_{\rm sys}$, we consider the exciton-photon-phonon coupling to second-order Born approximation, and trace over the phonon degrees of freedom to obtain a time convolutionless master equation [14, 32]:

$$\frac{\partial\rho}{\partial t} = \frac{1}{i\hbar}[H'_{\rm sys},\rho(t)] + \mathcal{L}(\rho) - \frac{1}{\hbar^2}\int_0^\infty d\tau \sum_{m=g,u}\Big(G_m(\tau) \times [\hat{X}_m, e^{-iH'_{sys}\tau/\hbar}\hat{X}_m e^{iH'_{sys}\tau/\hbar}\rho(t)] + \text{H.c}\Big), \qquad \textbf{(S7)}$$

where Lindblad operator terms, $\mathcal{L}(\rho)$, are the same as in the main text, and the polaron Green functions, which are obtained by tracing of the phonon degrees of freedom, are given by [8, 15], $G_g(t) = \langle B\rangle^2(\cosh[\phi(t)] - 1), G_u(t) = \langle B\rangle^2\sinh[\phi(t)]$, and the phonon correlation function, $\phi(t) = \int_0^\infty d\omega\frac{J(\omega)}{\omega^2}[\coth(\hbar\omega/2k_BT)\cos(\omega t) - i\sin(\omega t)]$. In practise, the phonon non-Markovian (memory) effects are extremely short timescale phenomena, and one can solve the above by replacing $t\to\infty$ in the integral [14, 32]. Thus we solve a Markovian master equation where the laser-dressed eigenvalues locally sample the phonon bath at different pump-dependent spectral locations.

A. Exciton driving with an off-resonant pump field

We now asses the influence of phonon-induced scattering on our previously described multiphoton effects. In Fig. S1 (and also shown as Fig. 10 of the main paper) we examine the cavity-emitted spectrum that can be compared to Fig. 7 of the main text—which described the multiphoton contribution to the pair of peaks centered near $\omega = \omega_L + 5g$. For clarity, we have absorbed the polaron shift, Δ_P, into the definition of ω_x. Here (with phonon interactions) the spectrum is calculated for a smaller pump power which results in a pair of more clearly separated peaks, which are expected to cross at approximately $\eta_x = 5g$. The effects of phonons are explored with these spectra for a phonon bath temperature of 4 K. We retain the bare coupling strength, g, and pump power, η_x (for ease of comparison to previous figures); however, all of these are now coherently renormalized (through the polaron transform) by $\langle B\rangle$ though this renormalization at 4 K is small ($\langle B\rangle = 0.96$). As a consequence of electron-phonon coupling, we observe a general broadening of all spectral features (EID), and an enhancement of the peak located at the cavity emission energy. These

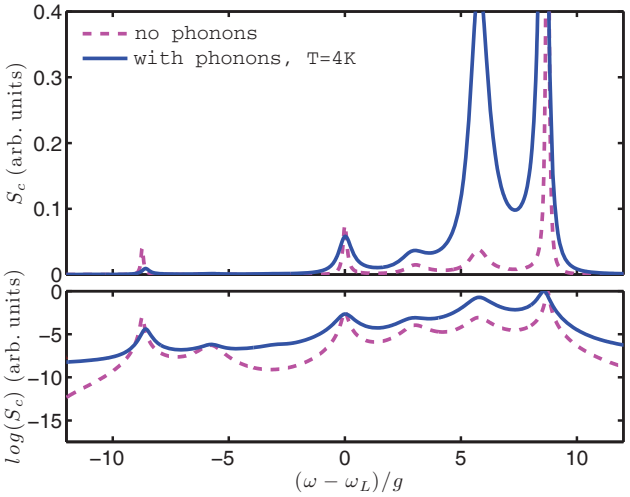

Fig. S1. Cavity-emitted spectra with an exciton drive, demonstrating the effects of phonon scattering at 4 K for parameter set-A in the main text ($\Gamma_c = g, \Gamma_x = g/100, \Gamma' = g/50$), with an excitation pump power of $\eta_x = 3g$ with a detuning of $\Delta_L = 6g$. All spectra have been normalized to 1.

effects are further amplified with increased temperatures (not shown), and, from the master equations, they generally scale with η_x^2 (EID) and g^2 (causing phonon-mediated exciton cavity coupling or feeding). Importantly, for a temperature of 4 K, all of the peaks present in the no phonon picture remain visible. In fact, a log plot of the spectrum demonstrates that even peaks that are not readily visible with a linear scale in the no-phonon spectra are not necessarily lost due to interactions with acoustic phonons.

Having established that it is possible to identify relevant peaks, even with phonon-induced broadening for at least one spectrum near a crossing of peaks with significant multiphoton contributions, we now examine the more general case. In Fig. S2, we present a plot of the cavity-emitted PL spectra as a function of pump power for parameter set-A with the phonons bath at a temperature of 4 K. We again retain the original g and η_x, and allow them to be renormalized by $\langle B \rangle = 0.96$, as appropriate. This figure can be compared and contrasted to the plot in Fig. 6 of the main text, which presents the same calculations without explicitly including phonon contributions. Upon comparison, we observe an overall broadening of the spectral features, which results in the visibility of fewer peaks. However, even upon the inclusion of phonons, there is still a clear deviation from the JC-WEA results—which are represented by dashed black lines overlaid upon the image. In particular, the phonon bath serves to strengthen the peak that is consistently present at the cavity frequency, ω_c—which is one of the deviations we observed from the JC-WEA. Additionally, it is still possible, though more challenging, to observe the crossing that takes place at a pump power of approximately $\eta_x = 5g$. This is highlighted in the lower panel of the figure, in which transition lines calculated using a two excitation approximation are overlaid over the image as a visual guide. As a note, we have found these results to be robust for detunings ranging from $\Delta_L = 3g$ to $\Delta_L = 10g$, with larger pump-cavity detunings being more favourable. Additionally, the sign of Δ_L has no significant qualitative effects on our results. Detuning the cavity to the opposite side of the laser decreases the oscillator strength of the peaks on

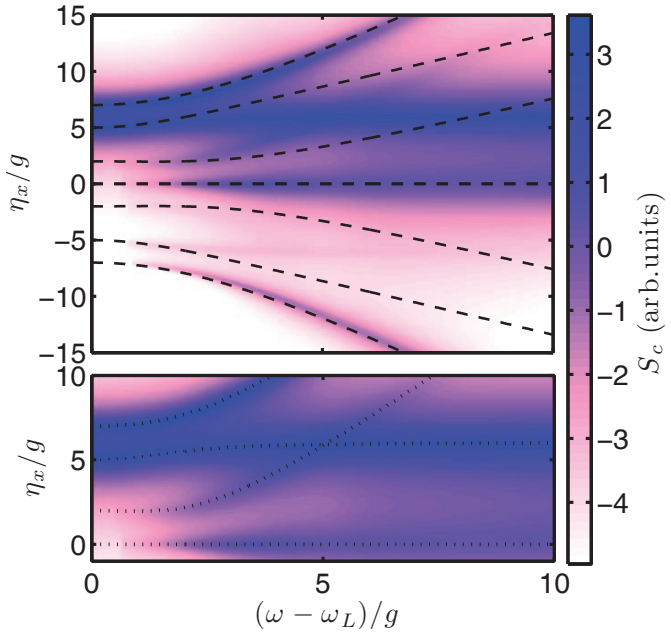

Fig. S2. $N-$photon spectral map (plotting the log of the cavity emitted spectra for a range of QD excitation energies). Phonons are included at a temperature of 4 K, and the calculation is done using parameter set-A with a detuning of $\Delta_L = 6g$. The dashed curves in the upper panel show the transition energies calculated in the JC-WEA (see main paper), and the dotted curves in the lower panel show a relevant subset of the transitions calculated in the two excitation approximation. Transitions not associated with visible peaks are ignored for the two excitation approximation for visual clarity.

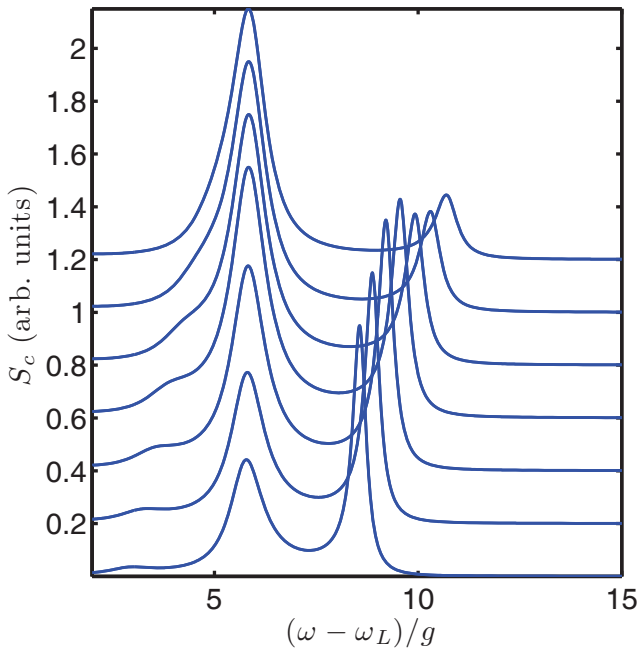

Fig. S3. Cavity-emitted spectra for parameter set-A with phonons at a temperature of 4 K. From bottom to top, the pump powers range from $\eta_x = 3g \rightarrow 4.5g$ in increments of $0.25g$. The detuning is $\Delta_L = 6g$ and all spectra have been normalized to 1.

the weaker half of the spectrum, with only small quantitative effects in the region of interest (not shown).

Since it is difficult to clearly view the crossing of interest using a spectral map, we examine it more closely by presenting spectra for a range of pump power from $3g$ to $4.5g$, in increments of $0.25g$ in Fig. S3. These spectra clearly show a strong peak at the cavity frequency $\omega_c = \omega_L + 6g$, as well as a smaller peak that begins to merge with it from lower energy. The phonon-induced broadening prevents clear observation of the smaller peak after the crossing is completed (not shown).

Modification of the Hamiltonian to include the effects of electron-acoustic phonon interactions—and thereby make a more direct connection to realistic semiconductor systems—has provided extra insight into the visibility of multiphoton effects in realistic QD systems. In particular, we found that the presence of the phonon bath leads to an enhancement of the peak at the cavity emission energy as well as a general spectral broadening of all peaks, similar to what happens for the recent prediction of phonon-dressed Mollow triplets [14]. The first of these effects emphasizes the difference in the pump power dependence of the $N-$photon versus the WEA results by enhancing one of the peaks that deviates most strongly from WEA behaviour. The latter diminishes the ability to observe all spectral features, making it more difficult to observe these effects. In general, the phonon induced broadening was not significant enough to wash out all spectral features for temperatures around 4 K, and therefore the deviations from the WEA result, though less prominent, still appear to be observable in the presence of the phonon bath. Further optimization of the parameters would likely make these multi-photon signatures even more pronounced.

B. Cavity driving with an off-resonant pump field

Near the end of section 3 in the main paper we examined multiphoton effects for cavity driven systems, for parameters appropriate for describing semiconductor systems. Here, we include the effects of electron-acoustic phonon coupling to the $N-$th order and verify that the multiphoton effects we predict are retained with this more complete theoretical treatment.

An $N-$photon spectral map calculated for a temperature of 4 K is presented in Fig. S4. This can be compared to the spectral map of Fig. 8 of the main text in which the same parameters were used, without accounting for the presence of phonons. As before, both cavity and excitonic emissions are shown. No significant modifications are observed on this level, primarily since EID is not expected to effect cavity driven systems—which was the primary source of phonon induced effects. We note that the deviations we previously noted from the JC-WEA are still clearly visible.

In order to observe the extent of the modifications resulting from the inclusion of phonons, we select a spectrum with an excitation energy of $\eta_c = 6g$, which falls in a regime in which significant deviations from the JC-WEA should be observable. In Fig. S5 (also shown as Fig. 11 in the main paper), we present this spectra at a phonon bath temperature of 4 K, as well as the equivalent spectrum calculated without the presence of the phonon bath. We observe that phonons now have a significantly less dramatic effect on the spectra for a cavity-driven system, in contrast to the QD-driven systems examined above. In particular, they only have a minor perturbation on the multiphoton spectral peaks.

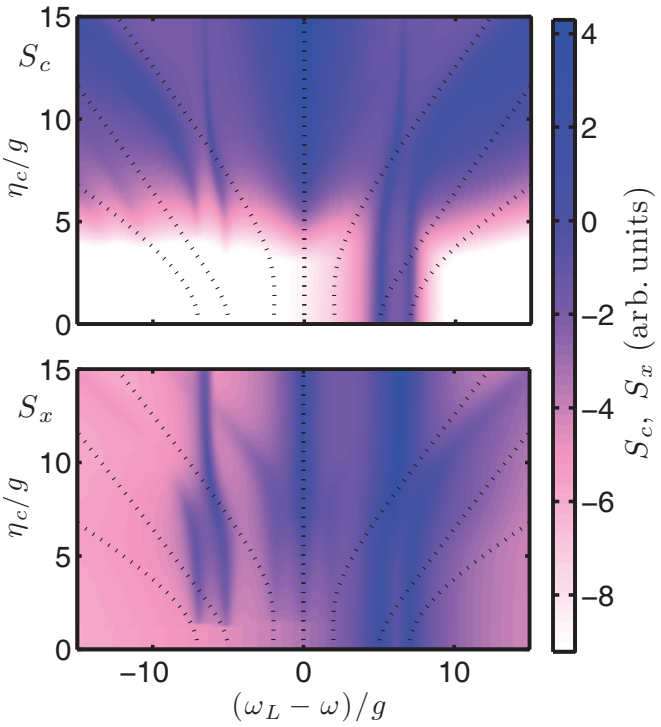

Fig. S4. Cavity emitted and exciton emitted $N-$photon spectral map (plotting the log of the cavity emitted spectra for a range of excitation energies) for a cavity driven system. Phonons are included at a temperature of 4 K, and the calculation is done using parameter set-A with a detuning of $\Delta_L = 6g$. The dashed curves show the transition energies calculated in the JC-WEA.

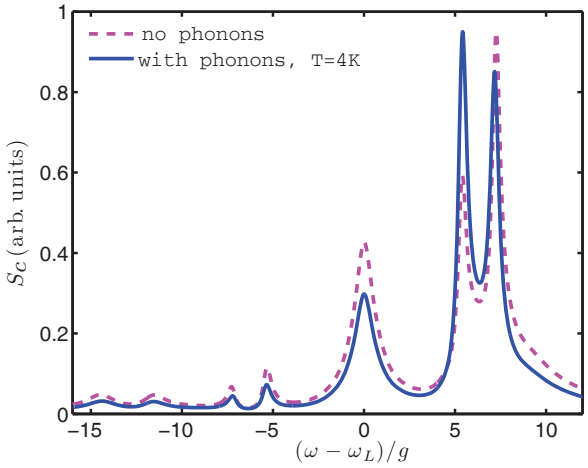

Fig. S5. Cavity-emitted spectra for a cavity driven system, demonstrating the effects of phonon scattering at 4 K for parameter set-A, with an excitation pump power of $\eta_x = 6g$ and $\Delta_L = 6g$.

REFERENCES

1. e.g., see R. W. D. Nickalls, "A new approach to solving the cubic: Cardan's solution revealed," The Mathematical Gazette **77**, 354 (1993).
2. T. Calarco, A. Datta, P. Fedichev, E. Pazy, and P. Zoller,

Phys. Rev. A **68**, 012310 (2003).
3. L. Besombes, K. Kheng, L. Marsal, and M. Mariette, Phys. Rev. B **63**, 155307 (2001).
4. E. Peter, J. Hours, P. Senellart, A. Vasanelli, A. Cavanna, J. Bloch, J. M. Gérard, Phys. Rev. B **69**, 041307 (2004).
5. I. Favero, G. Cassabois, R. Ferreira, D. Darson, C. Voisin, J. Tignon, C. Delalande, G. Bastard, Ph. Roussignol, and J. M. Gérard, Phys. Rev. B **68**, 233301 (2003).
6. A. Vagov, V. M. Axt, and T. Kuhn, Phys. Rev. B **66**, 165312 (2002).
7. J. Förstner, C. Weber, J. Danckwerts, and A. Knorr, Phys. Rev. Lett. **91**, 127401 (2003).
8. G. Mahan, Many-Particle Physics Plenum, New York, 1981.
9. B. Krummheuer, V. M. Axt, and T. Kuhn, Phys. Rev. B **65**, 195313 (2002).
10. D. Mogilevtsev, A. P. Nisovtsev, S. Kilin, S. B. Cavalcanti, H. S. Brandi, and L. E. Oliveira, Phys. Rev. Lett. **100**, 017401 (2008).
11. A. J. Ramsay, Achanta Venu Gopal, E. M. Gauger, A. Nazir, B. W. Lovett, A. M. Fox, and M. S. Skolnick, Phys. Rev. Lett. **104**, 017402 (2010).
12. A. J. Ramsay, T. M. Godden, S. J. Boyle, E. M. Gauger, A. Nazir, B. W. Lovett, A. M. Fox, and M. S. Skolnick, Phys. Rev. Lett **105**, 177402 (2010).
13. A. Nazir, Phys. Rev. B **78**, 153309 (2008).
14. C. Roy and S. Hughes, Phys. Rev. Lett. **106**, 247403 (2011).
15. I. Wilson-Rae and A. Imamoglŭ, Phys. Rev. B **65**, 235311 (2002).
16. F. Milde, A. Knorr, and S. Hughes, Phys. Rev. B **78**, 035330 (2008).
17. S. Hughes, P. Yao, F. Milde, A. Knorr, D. Dalacu, K. Mnaymneh, V. Sazonova, P. J. Poole, G. C. Aers, J. Lapointe, R. Cheriton, and R. L. Williams, Phys. Rev. B, 83, 165313 (2011).
18. Y. Ota, S. Iwamoto, N. Kumagai, and Y. Arakawa, e-print: arXiv:0908.0788v1 (2009).
19. S. M. Ulrich, S. Ates, S. Reitzenstein, A. Löffler, A. Forchel, and P. Michler, Phys. Rev. Lett **106**, 247402 (2011).
20. M. Calic, P. Gallo, M. Felici, K. A. Atlasov, B. Dwir, A. Rudra, G. Biasiol, L. Sorba, G. Tarel, V. Savona, and E. Kapon, Phys. Rev. Lett. **106**, 227402 (2011)
21. J. Xue, K-D Zhu and H. Zheng, J. Phys. C **20**, 3252009 (2008).
22. U. Hohenester, A. Laucht, M. Kaniber, N. Hauke, A. Neumann, A. Mohtashami, M. Selinger, M. Bichler, and J. J. Finley, Phys. Rev. B **81**, 201311 (2009).
23. P. Kaer, T. R. Nielsen, P. Lodahl, A.-P. Jauho, and J. Mørk, Phys. Rev. Lett. **104**, 157401 (2010).
24. J. Suffczynski, A. Dousse, K. Gauthron, A. Lemaitre, I. Sagnes, L. Lanco, J. Bloch, P. Voisin, and P. Senellart, Phys. Rev. Lett. **103**, 027401 (2009).
25. A. Majumdar, E. D. Kim, Y. Gong, M. Bajcsy, and J. Vučković, Phonon mediated off-resonant quantum dot–cavity coupling under resonant excitation of the quantum dot. Phys. Rev. B **84,** 085309 (2011).
26. Ata Ulhaq, Stefanie Weiler, Sven Marcus Ulrich, Michael Jetter, and Peter Michler, C. Roy, and S. Hughes, Optics Express, **21**, 4382 (2013).
27. S. Weiler., A. Ulhaq, S. M. Ulrich, D. Richter, M. Jetteri, P. Michler, C. Roy, and S. Hughes, Phys. Rev. B Rapid Communications **86**, 241304 (2012).
28. S. Hughes and H. J. Carmichael, N. J. Phys. **15**, 053039 (2013).
29. J.H. Quilter, A.J. Brash, F. Liu, M. Glässl, A. M. Barth, V.M. Axt, A.J. Ramsay, M.S. Skolnick, and A.M. Fox, Phys. Rev. Lett. **114**, 137401 (2015).
30. S. Hughes and H.J. Carmichael, Viewpoint: Crystal Vibrations Invert Quantum Dot Exciton, Physics 8, 29 (2015).
31. T. Calarco, A. Datta, P. Fedichev, E. Pazy, and P. Zoller, Phys. Rev. A **68**, 012310 (2003).
32. D. P. S. McCutcheon and A. Nazir, New J. Phys. **12**, 113042 (2010).